Bacillus subtilis-mediated weathering of basalt revealed through sporulation

AUTHOR NAMES

Christopher Yip[1], Kira Stonkevitch[1,#], Abigail Knecht[1,#], Philip D. Weyman[1], Tania Timmermann[1], Gonzalo A. Fuenzalida-Meriz[1,*]

AUTHOR ADDRESS

[1] Andes Ag, Inc., Alameda, CA, USA

[*]Corresponding author: Gonzalo A. Fuenzalida-Meriz, gonzalofuenzalida@gmail.com

[#]KS and AK contributed equally to this manuscript

ABSTRACT

Silicate rock weathering is a naturally occurring process that provides a long-term sink for atmospheric CO_2, but its natural rates are too slow on human-relevant timescales to offset anthropogenic emissions. Microbial activity offers a potential mechanism for accelerating silicate mineral dissolution and subsequent CO_2 drawdown. Here, we investigated the role of *Bacillus subtilis* strains MP1 and MP2 in the weathering of basalt, a cation-bearing, silicate-rich rock. Incubation of basalt with MP1 or MP2 resulted in significantly increased levels of soluble calcium compared to uninoculated, abiotic controls. In addition to calcium, we demonstrated that other metals released during basalt weathering can efficiently trigger sporulation. Because sporulation is known to require cations including Ca^{2+}, $Fe^{2/3+}$, and Mn^{2+}, this physiological response could be used as an additional proxy for monitoring and assessing silicate weathering in *in vitro* systems. Scanning electron microscopy revealed feldspar twinning features on basalt surfaces following

microbial treatment, providing concrete evidence of silicate rock weathering; these micrographs also identified numerous ovoid cell structures, indicating the presence of bacterial spores at the mineral surface. Together, these findings establish MP1 and MP2 as active agents of basalt weathering and highlight *Bacillus* sporulation as a potential biosensor for silicate dissolution. By linking microbial physiology with geochemical processes, our results highlight how strain-specific interactions with rock compositions could inform silicate weathering strategies for carbon dioxide removal (CDR), including Enhanced Weathering (EW) and Microbial Carbon Dioxide Mineralization (MCM).

1. INTRODUCTION

Silicate weathering is a fundamental geochemical process that regulates Earth's carbon cycle and has been central in stabilizing the global climate over millennia by generating a sink for carbon dioxide (CO_2) (Brantley et al., 2023; Trapp-Müller et al., 2025; Walker et al., 1981). In the weathering process and at the most basic level, silicate minerals found ubiquitously throughout terrestrial environments react with a variety of acids, including organic acids from microbial and plant origin, and carbonic acid formed from atmospheric CO_2 and water (Goll et al., 2021; Hartmann et al., 2013). Weathering liberates soluble metal cations from native silicates, and alkalinity is generated as a result of this process (Goll et al., 2021; Hartmann et al., 2013; Trapp-Müller et al., 2025). The resulting alkalinity is enriched for soluble bicarbonates and carbonates, and is transported through the soil column, eventually reaching the oceans, where it is estimated to be stable for thousands of years (Middelburg et al., 2020; Monger et al., 2015). As such, silicate weathering ultimately captures and removes atmospheric CO_2 and stores the carbon as stable carbonates and bicarbonates across geological timescales.

Because rates of silicate weathering are too slow to meaningfully counteract anthropogenic CO_2 emissions on timescales relevant to climate mitigation, new applications, practices, and technologies that facilitate more rapid silicate weathering are urgently needed, in combination with reducing CO_2 emissions themselves. In recent years, enhanced weathering (EW) has emerged as a promising strategy for CO_2 removal by applying silicate minerals to soils (Dietzen et al., 2018; Hasemer et al., 2024; Holzer et al., 2023; Kantola et al., 2023; Larkin et al., 2022). Supplementation of soils with crushed silicate minerals can mitigate soil acidification, and the increased mineral surface area accelerates silicate weathering and subsequent carbon dioxide

removal (CDR). Among the potential EW feedstocks, basaltic rocks are of particular interest. Basalt is one of the most abundant volcanic rocks on Earth and is rich in silicate minerals such as olivine, pyroxene, and plagioclase (Brooks, 2022). The widespread availability of basalt and its capacity to release divalent cations (e.g. Ca^{2+} and Mg^{2+}) make it an attractive candidate for large-scale deployment in agricultural settings for CDR efforts (Lewis et al., 2021). In addition to their ability to complex with and stabilize bicarbonate ions, the cations released by weathering have many co-benefits, including improving soil pH, soil fertility, and plant health (Sanderman, 2012; Wilson, 2004).

An alternative strategy to EW is the addition of specific microorganisms to soils that are already rich in cation-bearing silicate minerals (Timmermann et al., 2025). This strategy, termed microbial carbon dioxide mineralization (MCM), leverages naturally-occurring microbes, specifically their cellular processes and metabolisms, to accelerate and enhance the dissolution of native silicates without requiring additional rock applications. Microorganisms, particularly bacteria and fungi, are increasingly being recognized as active participants in silicate weathering (Finlay et al., 2020; Timmermann et al., 2025; Uroz et al., 2009; Vicca et al., 2022; Wild et al., 2022; Yang et al., 2026). Microbes and microbial communities can increase silicate dissolution rates relative to abiotic processes by altering the local pH and redox conditions (Mo & Lian, 2011; Timmermann et al., 2025). These microbes and microbial communities can also produce and secrete diverse panels of biomolecules such as organic acids, chelators, enzymes, and various other redox-active metabolites (Ahmed & Holmström, 2014; Basak & Biswas, 2009; Finlay et al., 2020; Ribeiro et al., 2020; Uroz et al., 2009; Vicca et al., 2022). Among the microbes that promote weathering, *Bacillus* species have attracted considerable attention for their ability to colonize mineral surfaces

and mobilize silicate-bound nutrients (Štyriaková et al., 2012). *B. mucilaginosus* and *B. edaphicus* are known to produce low molecular weight organic acids (e.g. oxalic and citric acids) that solubilize potassium and silicon from aluminosilicate-minerals, providing plant nutrients and improving soil fertility (Basak & Biswas, 2009; Han et al., 2025; Sheng, 2005).

Despite the growing evidence of microbial contributions to silicate rock weathering, far less is currently understood about how these interactions can subsequently affect microbial physiology (Ribeiro et al., 2020; Uroz et al., 2009). Many cellular processes are influenced by metal availability, including sporulation, and the ways microbes influence and respond to silicate weathering remain largely unexplored. Understanding physiological responses may reveal biological indicators for tracking microbially-mediated silicate weathering and could couple biochemical processes to CDR strategies.

We previously reported that *B. subtilis* strain MP1 (herein referred to as "MP1") enhanced the weathering of anorthite, a calcium rich feldspar, and promoted the formation of soil inorganic carbon under both laboratory and field conditions (Timmermann et al., 2025). A recent soil mesocosm study demonstrated that MP1 also improved the weathering of basalt, resulting in a significant increase in soil alkalinity (Yang et al., 2026). These findings established MP1 as an effective biological agent of silicate weathering and provided foundational evidence that microbial activity can drive silicate mineral dissolution and subsequent carbon dioxide removal in agricultural soils. MP1, however, is not genetically tractable, limiting genetic approaches to understanding the biochemical mechanisms of action of microbial-mediated silicate weathering. To overcome this limitation, we employed *Bacillus subtilis* strain MP2 (herein referred to as

116 "MP2"). MP2 shares approximately 99% DNA sequence similarity to MP1, but can be readily
117 modified using standard genetic tools. The close genetic relatedness between MP1 and MP2
118 enables direct comparison of their weathering capabilities while facilitating the generation of
119 defined mutants to interrogate weathering-associated cellular processes. Accordingly, MP2 serves
120 as a genetically tractable surrogate for MP1, enabling mechanistic analyses of *Bacillus*-mediated
121 silicate weathering.
122
123 In line with our previous findings, when calcium release was measured as a proxy for silicate
124 weathering under *in vitro* conditions, we consistently observed a decrease in soluble calcium at
125 later timepoints (Timmermann et al., 2025). We speculated that the decrease in calcium levels
126 could be due to the onset of sporulation, a cellular process requiring uptake of calcium, and/or the
127 precipitation of insoluble calcium carbonates. Consistent with this, high spore titers were
128 recovered from our established *in vitro* weathering assays and scanning electron microscopy
129 revealed basalt surfaces were heavily populated with *Bacillus* spores. Given that spore formation
130 in *B. subtilis* requires metals such as Ca^{2+}, $Fe^{2/3+}$, and Mn^{2+}, which are also found abundantly in
131 rocks such as basalt, we hypothesized that sporulation may act as an additional proxy for
132 microbially-mediated silicate weathering (Granger et al., 2011). Altogether, this study provides
133 new insight into the physiological responses of *B. subtilis* during silicate weathering and suggests
134 that sporulation may serve as a biological indicator of mineral dissolution. Furthermore, the
135 microbe's ability to procure the metals needed for sporulation from the rock is evidence of its
136 ability to promote rock weathering. By linking microbial metabolism and physiology to basalt
137 weathering dynamics, our findings expand the understanding of microbial contributions to
138 enhanced weathering and offer a framework for developing biologically informed CDR strategies.

2. MATERIALS AND METHODS

2.1. Isolation and identification of strain MP2. *Bacillus subtilis* strain MP2 is a naturally occurring soil microbe isolated from bunchgrass roots and rhizosphere soil samples from Imperial County, California, USA. Root samples with rhizosphere soil attached were collected and stored in a clean plastic bag. Soil and roots were divided into two samples (roots and rhizosphere soil), and portions of each sample were plated on LB-Lennox agar medium (1% tryptone, 0.5% yeast extract, 0.5% NaCl, 1.5% agar). MP2 was recovered as colonies from both rhizosphere soil and root samples.

Genome sequencing of MP2 was performed by Macrogen, Inc. (South Korea) using both PacBio and Illumina reads, and the resulting assembled genome was annotated with Bakta (Schwengers et al., 2021). MP1 and MP2 genomes were aligned with Mauve embedded in the Geneious Prime software package (version 2025.1.2) and were found to have a pairwise identity of 99.1%. MP1 and MP2 each share 86% pairwise identity with the common reference strain *Bacillus subtilis* subsp. *subtilis* strain 168.

2.2. Generation of Δ*spoIIE* mutant.

A deletion of the open reading frame (ORF) encoded by gene *spoIIE* was generated using homologous recombination in strain MP2. First, a plasmid was constructed using Gibson Assembly that consisted of 1) a 985-bp left homology region upstream of the *spoIIE* ORF that ended 15-bp before the start codon, 2) a 1230-bp spectinomycin cassette that was ordered as a gblock, 3) a 930-bp right homology region downstream of the *spoIIE* ORF and including the last

5-bp of the *spoIIE* ORF sequence, and 4) the vector pBR322 replacing the tetracycline resistance gene. Primers for the left homology region were 5'-TCCTAATGCATGTCTTCCGAGCTGGCAAGTAGCCTTGTTGACAC and 5'-ATATGTAAGATTTAAATGCAACCGCCTGTTATATTCGTTGCCTGT. Primers for the right homology region were 5'-AATAGGGGGATCTTCTCGAGATAACATAACGCTTCCGTATAAATCA and 5'-TGCTCACGTCAGTCCCATCGACGTTTCTGCCAAATACACAATTCC. The plasmid was sequenced and transformed into MP2 using natural transformation protocols and selection with spectinomycin (Hoover et al., 2010). Correct insertion was confirmed by PCR amplification of the entire left homology-spectinomycin resistance-right homology region from primers outside the homology arms and sequencing using Nanopore. The sporulation deficient phenotype was verified by the lack of spores after culturing in Difco Sporulation Medium.

2.3. Basalt preparation for weathering assays. Commercially available basalt (BrixBlend, from Pioneer Valley, MA, Fedcoseeds.com) was sieved to <710 µm particles using a no. 25 test sieve (VWR# 57334-268). Detailed mineral and elemental compositions can be found in supplemental tables S1 and S2. To remove available cations and easily weatherable carbonates, 60 g sieved basalt was resuspended in 600 ml 1 mM HCl and incubated at room temperature for 5 minutes. The basalt was then pelleted at 2000 x g for 5 minutes and the supernatant was decanted and discarded. The basalt pellet was washed an additional time with HCl, followed by two additional washes with distilled water. The basalt was then dried overnight at 60 °C, then sieved an additional time through a no. 25 test sieve.

2.4. Strain growth conditions, *in vitro* weathering assay, and analysis. *B. subtilis* strain MP1 and *B. subtilis* MP2-derived strains were routinely cultured at 30 °C in LB-Lennox medium. Basalt *in vitro* weathering assays were conducted over 3- and 7-day time courses and performed as follows: Exponential phase cultures were back diluted into mB4-1 (0.2% yeast extract, 0.3% casamino acids, 0.5% glucose, pH 7.3) to a final OD_{600} of 0.1. Two milliliters of the cultures were transferred to 24-well plates with or without 50 mg substrates or acid-washed basalt. The plates were sealed with breathable membranes and incubated without shaking at 30 °C. At specified timepoints, the biofilms were disrupted, and the cultures were homogenized by repeated pipetting. Approximately 1.5 ml of the cultures were collected, pelleted, and 1 ml of the clarified supernatants were assayed for pH and soluble calcium. To measure pH, 199 µl of clarified supernatants was added to a 96-well plate, then mixed with 1 µl 0.5% phenol red for a final concentration of 0.0025%. The sample absorbances were measured at 570 nm, then fitted against a 12-point sigmoidal curve with standards ranging from pH 5 to pH 9. Soluble calcium, liberated as a byproduct of basalt weathering, was measured using the QuantiChrom™ Calcium Assay Kit (DICA-500, Bioassay Systems). Briefly, 5 µl of clarified supernatants was added to a 96-well plate, mixed with 100 µl QuantiChrom™ working solution, and incubated at room temperature for at least 3 minutes. In the presence of calcium, the QuantiChrom™ dye forms a blue-colored complex that absorbs maximally at 612 nm. The calcium concentrations are directly proportional to the intensity of the blue color and were calculated when fitted to a 12-point calibration curve with calcium chloride standards ranging from 0 mM to 4 mM.

2.5. Assessing sporulation. To assess the presence of spores and to determine the sporulation efficiency of our strains, 50 µl of homogenized cultures were mixed with 450 µl 1X PBS. The

samples were serially diluted and plated onto LB agar to obtain total cell counts. In parallel, the homogenized cultures were incubated at 80 °C for 20 minutes to remove any heat-labile vegetative cells and to purify spores. The heat-treated samples were allowed to cool, serially diluted, then plated onto LB agar to obtain total spore counts.

2.6. Preparation of spent media. Δ*spoIIE* was cultured in nutrient broth (Difco, NB) supplemented with 0.5% glucose, with or without acid-washed basalt for 3 days to allow for mineral dissolution. The samples were pelleted, and the supernatants were filter-sterilized to generate spent nutrient broth prepared without basalt ("-BA Spent NB"), or spent nutrient broth prepared with basalt ("+BA Spent NB"). MP2 and Δ*spoIIE* were then inoculated into either fresh nutrient broth (NB), -BA Spent NB, or +BA Spent NB, then incubated at 30 °C for 3 days.

2.7. One-month basalt weathering assay. Basalt (Ward's Scientific) disks were cut to 1.5 cm diameter and 0.3 cm thickness, polished using 400 grit silicon carbide, sonicated to remove particulates, then sterilized by autoclaving. The basalt disks were dried overnight at 60 °C before use. To visually observe weathering by our *B. subtilis* strains MP1, MP2, and Δ*spoIIE*, exponential phase cultures were back diluted into nutrient broth supplemented with 0.5% glucose to a final OD_{600} of 0.1. Thirty milliliters of the cultures were transferred to 50 ml-beakers containing a sterilized basalt disk. The beakers were sealed with breathable membranes and incubated at room temperature, with minimal agitation (80 rpm).

After 30-days, the culture supernatants were decanted and stored at room temperature for soluble calcium measurements and spore and total cell enumeration (Supplemental Table S3). The basalt

disks were gently rinsed three times with dH_2O. The basalt disks were dried overnight at 60 °C, carbon coated to a thickness of 15 nm, then imaged using a JEOL JSM IT800HL Scanning Electron Microscope (SEM). The SEM was equipped with a backscatter electron detector (BED) and a secondary electron detector (SED), and routinely operated at 10-20 kV.

3. RESULTS

3.1. *Bacillus subtilis* facilitates the weathering of basalt.

To determine the extent to which *Bacillus subtilis* strains MP1 and MP2 facilitate silicate weathering and mobilize cations, the microbes were cultured in liquid mB4-1 medium with and without basalt for seven days (Figure 1 and Supplemental Figure S1). At each timepoint, the cultures were sampled and analyzed for soluble calcium derived from basalt-associated mineral dissolution. In the uninoculated control containing basalt, calcium concentrations gradually increased to approximately 0.44 mM by day 7 (Figure 1, solid orange line). In contrast, MP1 and MP2 cultures released significantly ($p < 0.0001$) higher calcium in the presence of basalt, reaching approximately 1.8 mM and 1.1 mM on day 7, respectively (Figure 1, solid gray and green lines). In samples lacking basalt, soluble calcium measurements remained low, demonstrating that the soluble calcium increases are derived only from the basalt substrate (Figure 1, dashed lines). The elevated calcium observed in the treatment containing both microbes and basalt suggests the liberated calcium was likely a consequence of microbially-mediated weathering of basalt.

Compared to MP1 cultures grown with calcium-bearing feldspars, MP1 and MP2 exhibited strikingly similar pH dynamics when cultured with basalt (Timmermann et al., 2025, and Supplemental Figure S2). In the absence of basalt, MP1 and MP2 initially decreased the media pH

by day 1, then gradually raised the alkalinity to pH 7 by the end of the experimental time course (Supplemental Figure S2, dashed gray and green lines). In contrast, MP1 and MP2 co-cultured with basalt exhibited a subtle decrease in pH by day 1 but then caused a rapid increase in pH, which was eventually stabilized near pH 9 (Supplemental Figure S2, solid gray and green lines). Additionally, compared to MP1 cultures treated with calcium-bearing feldspars (Timmermann et al., 2025), in the presence of basalt, MP1, MP2, and Δ*spoIIE* also exhibited robust pellicle formation; biofilms and pellicle formation were absent from samples containing the mB4-1 media alone (Supplemental Figure S1).

3.2. *Bacillus subtilis* MP1 and MP2 can undergo sporulation in the presence of basalt. We consistently observed a decrease in soluble calcium after day 2 of our *in vitro* weathering experiments with both feldspar and basalt (Timmermann et al., 2025, and Figure 1, respectively). We hypothesized that this decrease could be partially attributed to the onset of sporulation and the formation of mature spores, which are known to take up calcium from the medium (Nishikawa & Kobayashi, 2021; Paidhungat et al., 2000; Sinnelä et al., 2021). To test this hypothesis, we quantified the total number of cells and spores from cultures grown in the presence and absence of basalt after three days of incubation (Figure 2). Approximately 10^7 CFU/ml total viable cells were recovered from MP1 and MP2 cultures grown without basalt. Under basalt-free conditions, spore-forming units were recovered at approximately 10^3 spores/ml for MP1 and 10^4 spores/ml for MP2. Contrary, in the treatments where basalt was added, the total viable cell counts remained similar; however, spore counts increased significantly by ~4-log and ~2.5-log for MP1 and MP2, respectively (Figure 2). This significant increase in the number of spores and consequently

276 sporulation efficiency suggests that the microbes can weather basalt rocks which releases metals
277 required for the induction of sporulation (e.g., Ca^{2+}, Mg^{2+}, K^{+}, Mn^{2+}, and $Fe^{2/3+}$).
278
279 To determine whether the decrease in soluble calcium was directly linked to the onset of
280 sporulation and mature spore formation, we generated and examined a Δ*spoIIE* sporulation-
281 deficient strain of MP2. The Δ*spoIIE* strain was unable to produce spores when cultured under
282 standard sporulation promoting conditions (Supplemental Figure S3). When tested in a basalt
283 weathering assay, Δ*spoIIE* exhibited robust vegetative growth, and the total viable cell counts of
284 the mutant were similar to MP1 and MP2 in both the presence and absence of basalt (Figure 2).
285 As expected, the Δ*spoIIE* strain was unable to produce spores in the presence or absence of basalt.
286 When Δ*spoIIE* was cultured in the presence of basalt, calcium levels remained elevated well
287 beyond day 2, a point at which MP1 and MP2 calcium levels begin to decline (Figure 1, solid blue
288 line). These results support our hypothesis that sporulation is partially responsible for the decline
289 in soluble calcium during the course of basalt weathering under our laboratory conditions, as
290 calcium levels remained significantly elevated with Δ*spoIIE* in comparison to its wild type, MP2
291 ($p < 0.0001$), and to MP1 ($p < 0.01$) (Figure 1).
292
293 **3.3. Mineral substrates lacking key metals cannot induce *Bacillus* sporulation.**
294 Difco Sporulation Medium (DSM), a standardized medium for producing *B. subtilis* endospores,
295 contains several cations, notably Ca^{2+}, $Fe^{2/3+}$, K^{+}, Mg^{2+}, and Mn^{2+}, that can induce spore formation
296 and allow for the formation of mature spores (Granger et al., 2011; Li et al., 2022; Weinberg,
297 1964). To test whether the presence of specific metals influences sporulation, MP2 cultures were
298 incubated for three days in mB4-1 medium with or without different mineral substrates (Figure 3).

299 Importantly, mB4-1 alone cannot efficiently trigger *Bacillus* sporulation due to the absence of
300 essential metals (Figure 1 and Figure 2). Given the heterogeneous mixture of silicates and silicate-
301 bound metals found in basaltic rocks, we hypothesized that the weathering of basalt could release
302 essential metals, such as Mn^{2+}, that can trigger sporulation. Alternatively, substrates that lack this
303 panel of essential metals should not significantly trigger sporulation.
304
305 MP2 cultures grown in the presence and absence of metal-bearing substrates exhibited similar total
306 viable cell counts (~10^7 CFU/ml, Figure 3). In the absence of substrate, we recovered
307 approximately 10^5 spores/ml from MP2 (sporulation efficiency <1%). Consistent with our
308 hypothesis, MP2 grown in the presence of basalt exhibited an approximate 2-log increase in the
309 number of spores, relative to the no-substrate control; this increase in spore count corresponded to
310 a sporulation efficiency of approximately 56%. In contrast, while total viable cell counts were
311 comparable to the no-substrate control and basalt sample, minimal spore formation (sporulation
312 efficiency <1%) was observed when MP2 was co-cultured with dolomite, a calcium-magnesium
313 rich carbonate mineral that lacks other metal cations required for sporulation. Consistent with our
314 strains' ability to weather minerals, MP1, MP2, and Δ*spoIIE* could also liberate calcium from
315 dolomite (Supplemental Figure S4). These findings demonstrate that sporulation of *Bacillus* strains
316 cannot be induced solely by the presence of soluble calcium or magnesium (as in the case with
317 dolomite), but instead relies on accessing a broader suite of trace metals released from silicate
318 substrates such as basalt.
319
320 **3.4. Basalt weathering by MP2 and Δ*spoIIE* releases soluble cations that induce sporulation.**

We next questioned whether *B. subtilis* co-cultured with basalt could reconstitute a spore-inducing medium from a medium that normally cannot trigger *Bacillus* sporulation. We hypothesized that MP2 and Δ*spoIIE* can weather basalt to release basalt-associated metals, to then trigger sporulation. To determine if the interaction between *B. subtilis* and basalt could generate weathering products (i.e., Ca^{2+}, $Fe^{2/3+}$, K^{+}, Mg^{2+}, and Mn^{2+}) capable of triggering sporulation in other cells, we assessed cell-free supernatants generated from Δ*spoIIE* grown in the presence and absence of basalt.

MP2 and Δ*spoIIE* grew to similar cell densities (~10^7 CFU/ml) across all three media treatments, indicating that growth was not limited by nutrient depletion in the spent media (Figure 4, purple). In fresh nutrient broth (NB)and spent nutrient broth lacking basalt (-BA Spent NB), MP2 exhibited minimal sporulation (approximately 10^2-10^3 spores/ml). Strikingly, MP2 grown in spent nutrient broth derived from Δ*spoIIE* cultured in the presence of basalt (+BA Spent NB) showed a drastic and significant ($p < 0.01$) increase in spore CFUs (Figure 4). This increase in spore counts corresponded to a sporulation efficiency of approximately 60%. As expected, we were unable to recover or detect any Δ*spoIIE* spores under any of the conditions tested. Together, these findings suggest that Δ*spoIIE* and MP2 can weather silicates to release soluble metal ions (Ca^{2+}, $Fe^{2/3+}$, Mn^{2+}, as well as other silicate-derived metals) into the surrounding medium, and these metals can induce sporulation in *B. subtilis* (Figures 2, 3, and 4).

3.5. Basalt surfaces incubated with MP1 and MP2 reveal feldspar twinning and are heavily populated with *Bacillus* spores.

After demonstrating the positive effects of MP1 and MP2 on basalt dissolution by measuring soluble calcium and sporulation efficiencies as proxies, we next examined whether the apparent weathering activity could manifest observable changes to basalt surfaces. To demonstrate this potential effect, we conducted scanning electron microscopy (SEM) analyses on polished basalt surfaces. In the absence of microbes, the uninoculated control (UTC) exhibited no microbial colonization (Figure 5 and Supplemental Figure S5). In contrast, basalt incubated with MP1 and MP2 were heavily colonized (Figure 5 and Supplemental Figure S5). Interestingly, no colonization was observed when the basalt was cultured with Δ*spoIIE* (Figure 5, '*ΔspoIIE'*). Although Δ*spoIIE* cells were not detected on basalt surfaces, viable cell counts were recovered after the 30-day incubation period (Supplemental Table S3). Δ*spoIIE*'s absence in these micrographs likely reflects differences in developmental stages (discussed later).

Upon closer examination of the cell morphologies at higher magnifications (2000x and 4000x), the basalt rocks were heavily populated with ovoid structures approximately 1 μm in length (Figure 5). The size and shape of these structures are consistent with *Bacillus subtilis* spores. In line with our datasets, approximately 10^7 spores/ml were recovered from MP1 and MP2 after the 30-day incubation (Supplemental Table S3). No spores were recovered from Δ*spoIIE* under these conditions. Interestingly, vegetative Δ*spoIIE* cells were also visually absent from the micrographs. It is possible the heat-labile Δ*spoIIE* were unable to survive the long incubation period (30 days) and/or the drying and downstream SEM sample preparation processes. Furthermore, it is also possible that *Bacillus* spores have additional adhesion factors that allow them to attach to and retain onto the basalt disks, whereas vegetative cells cannot.

Evidence of silicate weathering can often manifest as micropitting or etching on mineral surfaces (Lybrand et al., 2019; Song et al., 2007, 2010). As expected, we were unable to find evidence of weathering in our UTC sample, as pitting and etching were visually absent, and the mineral surfaces remained smooth. In contrast, we observed structured, striation-like features on the surfaces of the basalt disks incubated with MP1, MP2, and Δ*spoIIE* (Figure 5, red arrows). These features are likely twinning of feldspar minerals within the basalt rock, a phenomenon related to geometric crystalline growth. The presence and greater abundance of these features relative to the UTC sample suggests enhanced mineral dissolution driven by the microbes.

4. DISCUSSION

The positive effects of microbes on feldspar weathering prompted us to evaluate whether a similar phenomenon would occur with basaltic rocks. Importantly, the relatively high abundance, widespread availability, and capacity of basalt to release divalent cations relevant to carbon dioxide removal make it an attractive candidate for EW practices. To examine the effect of *B. subtilis* environmental isolates MP1 and MP2 on basalt weathering, we utilized a similar weathering screen as previously described (Timmermann et al., 2025). In uninoculated controls containing basalt, calcium concentrations gradually increased, which we attributed to abiotic dissolution and, potentially, the release of readily accessible surface ions. In contrast, MP1 and MP2, when co-cultured with basalt, solubilized and released three- to four-fold more calcium in comparison to uninoculated controls, indicating a substantial microbial enhancement of basalt dissolution.

Silicate weathering is widely recognized as a pH-dependent process (Brady & Walther, 1989; Hartmann et al., 2013; White & Brantley, 2003). Across all conditions tested, MP1, MP2, and Δ*spoIIE* initially decreased the media pH by day 1, independent of substrate type or substrate addition. However, in the presence of basalt, the cultures exhibited a very subtle decrease in pH, relative to cultures lacking substrate, which could be partially attributed to basalt acting as a sink for H^+. Silicate weathering, which consumes protons and thus raises pH, led to the release of base cations and alkalinity. As previously observed during feldspar weathering, we propose that these pH dynamics are also exaggerated and driven by microbial metabolism in response to cation-bearing silicate substrates and serve to promote mineral dissolution (Timmermann et al., 2025). Accordingly, both MP1 and MP2 enhanced the dissolution of basalt and the release of calcium above abiotic levels, which is consistent with microbially-mediated silicate weathering.

During silicate dissolution, the concentration of soluble metals and base cations is expected to increase over time and remain elevated. We consistently observed a decline in soluble calcium on or after day 2 with both anorthite and basalt during our *in vitro* weathering assays (Timmermann et al., 2025). There are at least two potential mechanisms for this decrease: the precipitation of carbonate minerals under alkaline conditions, and the uptake of calcium through cellular processes (sporulation and biofilm formation). Sporulation in *Bacillus* species is known to require substantial amounts of calcium and, in the presence of basalt, MP1 and MP2 exhibited significantly higher spore counts despite similar total viable cell counts relative to the no-substrate controls. In contrast, the Δ*spoIIE*-derivative of MP2 maintained comparable vegetative cell growth in the presence of basalt but was unable to form heat-resistant spores and did not exhibit a decrease in soluble calcium. These observations indicated that sporulation contributes to calcium depletion during

411 basalt weathering, although it is unlikely to be the sole sink for released calcium. Indeed, calcium
412 incorporated into spores accounted for only ~10% of the total calcium released, suggesting that
413 the majority of the weathered-derived cations remain available for downstream geochemical
414 processes, including carbonate and bicarbonate formation relevant to CDR strategies.
415
416 Having identified sporulation as a relevant sink for calcium during basalt weathering, we next
417 investigated whether sporulation could serve as a physiological proxy for silicate weathering in a
418 defined medium. Soluble calcium measurements provide useful geochemical evidence for
419 weathering activity but have some limitations. First, geochemical evidence does not provide
420 insight into the physiological responses of microbial cells to mineral-derived metals and, second,
421 they cannot discriminate between weathering of silicate versus non-silicate minerals (e.g., calcium
422 carbonates). Using alternative mineral substrates, we demonstrated that although MP1 and MP2
423 were capable of liberating calcium from dolomite, sporulation was not induced, indicating that
424 calcium and magnesium alone are insufficient to trigger this developmental response. Furthermore,
425 cell-free spent media generated from Δ*spoIIE* cultures incubated with basalt strongly induced MP2
426 sporulation, whereas spent media derived from Δ*spoIIE* grown without basalt had no such effect.
427 These findings confirm that Δ*spoIIE* was able to weather basalt and extract key elements such as
428 Mn^{2+} and $Fe^{2/3+}$ for the induction of sporulation, and Ca^{2+} for the formation of mature spores in *B.*
429 *subtilis*. Our findings suggest soluble products of basalt weathering can trigger sporulation and
430 that sporulation may serve as a complementary indicator for silicate weathering by *Bacillus*.
431
432 The soluble calcium measurements and presence of microbial spores under basalt treatment
433 provided complementary geochemical and physiological evidence for microbial-mediated

weathering of basalt. We therefore investigated whether this activity could also be accompanied by detectable physical changes to basalt surfaces. Twinning is a characteristic crystalline structure that can commonly occur in feldspar minerals and is formed from the intergrowth of two or more crystal lattices (Lee et al., 1998; Parsons et al., 2015). As these crystalline structures exist naturally within feldspars, we hypothesized that the dissolution of silicate minerals through weathering processes could expose underlying twinning structures. SEM analyses of basalt disks treated with MP1, MP2, and Δ*spoIIE* revealed prominent striation-like features that are consistent with feldspar twinning. Importantly, these features were conspicuously absent from uninoculated controls. The prevalence of twinning in the microbe-treated samples likely reflects overall mineral dissolution enhanced by the microbes. Thus, while twinning features are likely present in the original silicate rock samples, the increased visibility of these features in the presence of microbes is consistent with microbially-mediated weathering of basalt.

Collectively, these findings establish *Bacillus subtilis* MP1 and MP2 as active and effective biological agents capable of enhancing basalt weathering under controlled *in vitro* conditions. Beyond increased cation release, this work identifies sporulation as a sensitive physiological proxy for microbial access to mineral-derived metals and extends prior observations of microbially-mediated feldspar weathering to compositionally-complex and environmentally-relevant basalt rocks. The ability of *Bacillus* species to integrate mineral dissolution products into developmental processes highlights a tight coupling between microbial physiology and environmental geochemistry.

Future work should focus on identifying specific chemical species, biomolecules, and molecular mechanisms that mediate basalt dissolution by *Bacillus*. This information will be critical for understanding how these processes operate in soils and other natural environments. Determining how microbial physiology, mineral composition, and environmental conditions interact to regulate weathering rates will help guide biologically informed strategies for enhancing silicate weathering. Ultimately, integrating microbial processes into enhanced weathering frameworks (e.g., Yang et al., 2026) may provide a scalable and mechanistically grounded approach for accelerating carbon dioxide removal through microbially-mediated silicate dissolution.

ACKNOWLEDGMENTS

We thank John L. Grimsich at the University of California, Berkeley's Earth and Planetary Science Department (EPS) for their help preparing and processing the basalt disks, and for their expertise and technical support on the JEOL JSM IT800HL Scanning Electron Microscope. We also thank Marjorie Schulz for their advice interpreting SEM images and Corey R. Lawrence for their biogeochemical advice and feedback on the manuscript.

AUTHOR CONTRIBUTIONS

CY designed, planned, and managed the experiments. CY, KS, and AK performed the experiments and collected samples and data. TT, CY, PDW performed statistical analyses. CY, PDW, and TT wrote the first draft of the manuscript. GAFM and TT acquired funding for this study. All authors read, edited, and approved the final manuscript.

CONFLICTS OF INTEREST

The authors declare potential competing interests as follows: Christopher Yip, Kira Stonkevitch, Abigail Knecht, Philip D. Weyman, Tania Timmermann, and Gonzalo A. Fuenzalida-Meriz are employed by Andes Ag Inc., the company that funded this study.

REFERENCES

Ahmed, E., & Holmström, S. J. M. (2014). Siderophores in environmental research: roles and applications. *Microbial Biotechnology*, *7*(3), 196–208. https://doi.org/10.1111/1751-7915.12117

Basak, B. B., & Biswas, D. R. (2009). Influence of potassium solubilizing microorganism (Bacillus mucilaginosus) and waste mica on potassium uptake dynamics by sudan grass (Sorghum vulgare Pers.) grown under two Alfisols. *Plant and Soil*, *317*(1–2), 235–255. https://doi.org/10.1007/s11104-008-9805-z

Brady, P. V., & Walther, J. V. (1989). Controls on silicate dissolution rates in neutral and basic pH solutions at 25°C. *Geochimica et Cosmochimica Acta*, *53*(11), 2823–2830. https://doi.org/10.1016/0016-7037(89)90160-9

Brantley, S. L., Shaughnessy, A., Lebedeva, M. I., & Balashov, V. N. (2023). How temperature-dependent silicate weathering acts as Earth's geological thermostat. *Science*, *379*(6630), 382–389. https://doi.org/10.1126/science.add2922

Brooks, K. (2022). Rocks explained 2: Basalt. *Geology Today*, *38*(6), 236–242. https://doi.org/10.1111/gto.12414

Dietzen, C., Harrison, R., & Michelsen-Correa, S. (2018). Effectiveness of enhanced mineral weathering as a carbon sequestration tool and alternative to agricultural lime: An incubation

experiment. *International Journal of Greenhouse Gas Control*, *74*, 251–258. https://doi.org/10.1016/j.ijggc.2018.05.007

Finlay, R. D., Mahmood, S., Rosenstock, N., Bolou-Bi, E. B., Köhler, S. J., Fahad, Z., Rosling, A., Wallander, H., Belyazid, S., Bishop, K., & Lian, B. (2020). Reviews and syntheses: Biological weathering and its consequences at different spatial levels – from nanoscale to global scale. *Biogeosciences*, *17*(6), 1507–1533. https://doi.org/10.5194/bg-17-1507-2020

Goll, D. S., Ciais, P., Amann, T., Buermann, W., Chang, J., Eker, S., Hartmann, J., Janssens, I., Li, W., Obersteiner, M., Penuelas, J., Tanaka, K., & Vicca, S. (2021). Potential CO2 removal from enhanced weathering by ecosystem responses to powdered rock. *Nature Geoscience*, *14*(8), 545–549. https://doi.org/10.1038/s41561-021-00798-x

Granger, A. C., Gaidamakova, E. K., Matrosova, V. Y., Daly, M. J., & Setlow, P. (2011). Effects of Mn and Fe Levels on Bacillus subtilis Spore Resistance and Effects of Mn2+, Other Divalent Cations, Orthophosphate, and Dipicolinic Acid on Protein Resistance to Ionizing Radiation. *Applied and Environmental Microbiology*, *77*(1), 32–40. https://doi.org/10.1128/AEM.01965-10

Han, X., Shen, Y., Sun, L., Shen, J., Mao, Y., Fan, K., Wang, S., Ding, Z., & Wang, Y. (2025). Phyllospheric application of Bacillus mucilaginosus mediates the recovery of tea plants exposed to low-temperature stress by alteration of leaf endophytic community and plant physiology. *BMC Microbiology*, *25*(1), 177. https://doi.org/10.1186/s12866-025-03880-1

Hartmann, J., West, A. J., Renforth, P., Köhler, P., De La Rocha, C. L., Wolf-Gladrow, D. A., Dürr, H. H., & Scheffran, J. (2013). Enhanced chemical weathering as a geoengineering strategy to reduce atmospheric carbon dioxide, supply nutrients, and mitigate ocean acidification. *Reviews of Geophysics*, *51*(2), 113–149. https://doi.org/10.1002/rog.20004

524 Hasemer, H., Borevitz, J., & Buss, W. (2024). Measuring enhanced weathering: inorganic
525 carbon-based approaches may be required to complement cation-based approaches.
526 *Frontiers in Climate*, *6*. https://doi.org/10.3389/fclim.2024.1352825
527 Holzer, I. O., Nocco, M. A., & Houlton, B. Z. (2023). Direct evidence for atmospheric carbon
528 dioxide removal via enhanced weathering in cropland soil. *Environmental Research*
529 *Communications*, *5*(10), 101004. https://doi.org/10.1088/2515-7620/acfd89
530 Hoover, S. E., Xu, W., Xiao, W., & Burkholder, W. F. (2010). Changes in DnaA-Dependent
531 Gene Expression Contribute to the Transcriptional and Developmental Response of *Bacillus*
532 *subtilis* to Manganese Limitation in Luria-Bertani Medium. *Journal of Bacteriology*,
533 *192*(15), 3915–3924. https://doi.org/10.1128/JB.00210-10
534 Kantola, I. B., Blanc-Betes, E., Masters, M. D., Chang, E., Marklein, A., Moore, C. E., von
535 Haden, A., Bernacchi, C. J., Wolf, A., Epihov, D. Z., Beerling, D. J., & DeLucia, E. H.
536 (2023). Improved net carbon budgets in the <scp>US</scp> Midwest through direct
537 measured impacts of enhanced weathering. *Global Change Biology*, *29*(24), 7012–7028.
538 https://doi.org/10.1111/gcb.16903
539 Larkin, C. S., Andrews, M. G., Pearce, C. R., Yeong, K. L., Beerling, D. J., Bellamy, J.,
540 Benedick, S., Freckleton, R. P., Goring-Harford, H., Sadekar, S., & James, R. H. (2022).
541 Quantification of CO2 removal in a large-scale enhanced weathering field trial on an oil
542 palm plantation in Sabah, Malaysia. *Frontiers in Climate*, *4*.
543 https://doi.org/10.3389/fclim.2022.959229
544 Lee, M. R., Hodson, M. E., & Parsons, I. (1998). The role of intragranular microtextures and
545 microstructures in chemical and mechanical weathering: direct comparisons of

546 experimentally and naturally weathered alkali feldspars. *Geochimica et Cosmochimica*
547 *Acta*, *62*(16), 2771–2788. https://doi.org/10.1016/S0016-7037(98)00200-2
548 Lewis, A. L., Sarkar, B., Wade, P., Kemp, S. J., Hodson, M. E., Taylor, L. L., Yeong, K. L.,
549 Davies, K., Nelson, P. N., Bird, M. I., Kantola, I. B., Masters, M. D., DeLucia, E., Leake, J.
550 R., Banwart, S. A., & Beerling, D. J. (2021). Effects of mineralogy, chemistry and physical
551 properties of basalts on carbon capture potential and plant-nutrient element release via
552 enhanced weathering. *Applied Geochemistry*, *132*, 105023.
553 https://doi.org/10.1016/j.apgeochem.2021.105023
554 Li, L., Jin, J., Hu, H., Deveau, I. F., Foley, S. L., & Chen, H. (2022). Optimization of sporulation
555 and purification methods for sporicidal efficacy assessment on Bacillus spores. *Journal of*
556 *Industrial Microbiology and Biotechnology*, *49*(4). https://doi.org/10.1093/jimb/kuac014
557 Lybrand, R. A., Austin, J. C., Fedenko, J., Gallery, R. E., Rooney, E., Schroeder, P. A.,
558 Zaharescu, D. G., & Qafoku, O. (2019). A coupled microscopy approach to assess the nano-
559 landscape of weathering. *Scientific Reports*, *9*(1), 5377. https://doi.org/10.1038/s41598-019-
560 41357-0
561 Middelburg, J. J., Soetaert, K., & Hagens, M. (2020). Ocean Alkalinity, Buffering and
562 Biogeochemical Processes. *Reviews of Geophysics*, *58*(3).
563 https://doi.org/10.1029/2019RG000681
564 Mo, B., & Lian, B. (2011). Interactions between Bacillus mucilaginosus and silicate minerals
565 (weathered adamellite and feldspar): Weathering rate, products, and reaction mechanisms.
566 *Chinese Journal of Geochemistry*, *30*(2), 187–192. https://doi.org/10.1007/s11631-011-
567 0500-z

568 Monger, H. C., Kraimer, R. A., Khresat, S., Cole, D. R., Wang, X., & Wang, J. (2015).
569 Sequestration of inorganic carbon in soil and groundwater. *Geology*, *43*(5), 375–378.
570 https://doi.org/10.1130/G36449.1
571 Nishikawa, M., & Kobayashi, K. (2021). Calcium Prevents Biofilm Dispersion in Bacillus
572 subtilis. *Journal of Bacteriology*, *203*(14). https://doi.org/10.1128/JB.00114-21
573 Paidhungat, M., Setlow, B., Driks, A., & Setlow, P. (2000). Characterization of Spores of
574 Bacillus subtilis Which Lack Dipicolinic Acid. *Journal of Bacteriology*, *182*(19), 5505–
575 5512. https://doi.org/10.1128/JB.182.19.5505-5512.2000
576 Parsons, I., Fitz Gerald, J. D., & Lee, M. R. (2015). Routine characterization and interpretation
577 of complex alkali feldspar intergrowths. *American Mineralogist*, *100*(5–6), 1277–1303.
578 https://doi.org/10.2138/am-2015-5094
579 Ribeiro, I. D. A., Volpiano, C. G., Vargas, L. K., Granada, C. E., Lisboa, B. B., & Passaglia, L.
580 M. P. (2020). Use of Mineral Weathering Bacteria to Enhance Nutrient Availability in
581 Crops: A Review. *Frontiers in Plant Science*, *11*. https://doi.org/10.3389/fpls.2020.590774
582 Sanderman, J. (2012). Can management induced changes in the carbonate system drive soil
583 carbon sequestration? A review with particular focus on Australia. *Agriculture, Ecosystems*
584 *& Environment*, *155*, 70–77. https://doi.org/10.1016/j.agee.2012.04.015
585 Schwengers, O., Jelonek, L., Dieckmann, M. A., Beyvers, S., Blom, J., & Goesmann, A. (2021).
586 Bakta: rapid and standardized annotation of bacterial genomes via alignment-free sequence
587 identification. *Microbial Genomics*, *7*(11). https://doi.org/10.1099/mgen.0.000685
588 Sheng, X. F. (2005). Growth promotion and increased potassium uptake of cotton and rape by a
589 potassium releasing strain of Bacillus edaphicus. *Soil Biology and Biochemistry*, *37*(10),
590 1918–1922. https://doi.org/10.1016/j.soilbio.2005.02.026

591 Sinnelä, M. T., Pawluk, A. M., Jin, Y. H., Kim, D., & Mah, J.-H. (2021). Effect of Calcium and
592 Manganese Supplementation on Heat Resistance of Spores of Bacillus Species Associated
593 With Food Poisoning, Spoilage, and Fermentation. *Frontiers in Microbiology*, *12*.
594 https://doi.org/10.3389/fmicb.2021.744953
595 Song, W., Ogawa, N., Oguchi, C. T., Hatta, T., & Matsukura, Y. (2007). Effect of Bacillus
596 subtilis on granite weathering: A laboratory experiment. *CATENA*, *70*(3), 275–281.
597 https://doi.org/10.1016/j.catena.2006.09.003
598 Song, W., Ogawa, N., Takashima-Oguchi, C., Hatta, T., & Matsukura, Y. (2010). Laboratory
599 experiments on bacterial weathering of granite and its constituent minerals.
600 *Géomorphologie : Relief, Processus, Environnement*, *16*(4), 327–336.
601 https://doi.org/10.4000/geomorphologie.8038
602 Štyriaková, I., Štyriak, I., & Oberhänsli, H. (2012). Rock weathering by indigenous heterotrophic
603 bacteria of Bacillus spp. at different temperature: a laboratory experiment. *Mineralogy and*
604 *Petrology*, *105*(3–4), 135–144. https://doi.org/10.1007/s00710-012-0201-2
605 Timmermann, T., Yip, C., Yang, Y., Wemmer, K. A., Chowdhury, A., Dores, D., Takayama, T.,
606 Nademanee, S., Traag, B. A., Zamanian, K., González, B., Breecker, D. O., Fierer, N.,
607 Slessarev, E. W., & Fuenzalida-Meriz, G. A. (2025). Harnessing Microbes to Weather
608 Native Silicates in Agricultural Soils for Scalable Carbon Dioxide Removal. *Global Change*
609 *Biology*, *31*(5). https://doi.org/10.1111/gcb.70216
610 Trapp-Müller, G., Caves Rugenstein, J., Conley, D. J., Geilert, S., Hagens, M., Hong, W.-L.,
611 Jeandel, C., Longman, J., Mason, P. R. D., Middelburg, J. J., Milliken, K. L., Navarre-
612 Sitchler, A., Planavsky, N. J., Reichart, G.-J., Slomp, C. P., Sluijs, A., van Hinsbergen, D. J.

J., & Zhang, X. Y. (2025). Earth's silicate weathering continuum. *Nature Geoscience*, *18*(8), 691–701. https://doi.org/10.1038/s41561-025-01743-y

Uroz, S., Calvaruso, C., Turpault, M.-P., & Frey-Klett, P. (2009). Mineral weathering by bacteria: ecology, actors and mechanisms. *Trends in Microbiology*, *17*(8), 378–387. https://doi.org/10.1016/j.tim.2009.05.004

Vicca, S., Goll, D. S., Hagens, M., Hartmann, J., Janssens, I. A., Neubeck, A., Peñuelas, J., Poblador, S., Rijnders, J., Sardans, J., Struyf, E., Swoboda, P., van Groenigen, J. W., Vienne, A., & Verbruggen, E. (2022). Is the climate change mitigation effect of enhanced silicate weathering governed by biological processes? *Global Change Biology*, *28*(3), 711–726. https://doi.org/10.1111/gcb.15993

Walker, J. C. G., Hays, P. B., & Kasting, J. F. (1981). A negative feedback mechanism for the long-term stabilization of Earth's surface temperature. *Journal of Geophysical Research: Oceans*, *86*(C10), 9776–9782. https://doi.org/10.1029/JC086iC10p09776

Weinberg, E. D. (1964). Manganese Requirement for Sporulation and Other Secondary Biosynthetic Processes of Bacillus. *Applied Microbiology*, *12*(5), 436–441. https://doi.org/10.1128/am.12.5.436-441.1964

White, A. F., & Brantley, S. L. (2003). The effect of time on the weathering of silicate minerals: why do weathering rates differ in the laboratory and field? *Chemical Geology*, *202*(3–4), 479–506. https://doi.org/10.1016/j.chemgeo.2003.03.001

Wild, B., Gerrits, R., & Bonneville, S. (2022). The contribution of living organisms to rock weathering in the critical zone. *Npj Materials Degradation*, *6*(1), 98. https://doi.org/10.1038/s41529-022-00312-7

Wilson, M. J. (2004). Weathering of the primary rock-forming minerals: processes, products and rates. *Clay Minerals*, *39*(3), 233–266. https://doi.org/10.1180/0009855043930133

Yang, Y., Bueno de Mesquita, C. P., Lawrence, C. R., Weyman, P. D., Dores, D., Timmermann, T., Fierer, N., & Fuenzalida-Meriz, G. A. (2026). Synergistic Effects of a Microbial Amendment and Crushed Basalt: Soil Geochemical and Microbial Responses. *Global Change Biology*, *32*(1). https://doi.org/10.1111/gcb.70705

MAIN FIGURES AND TABLES

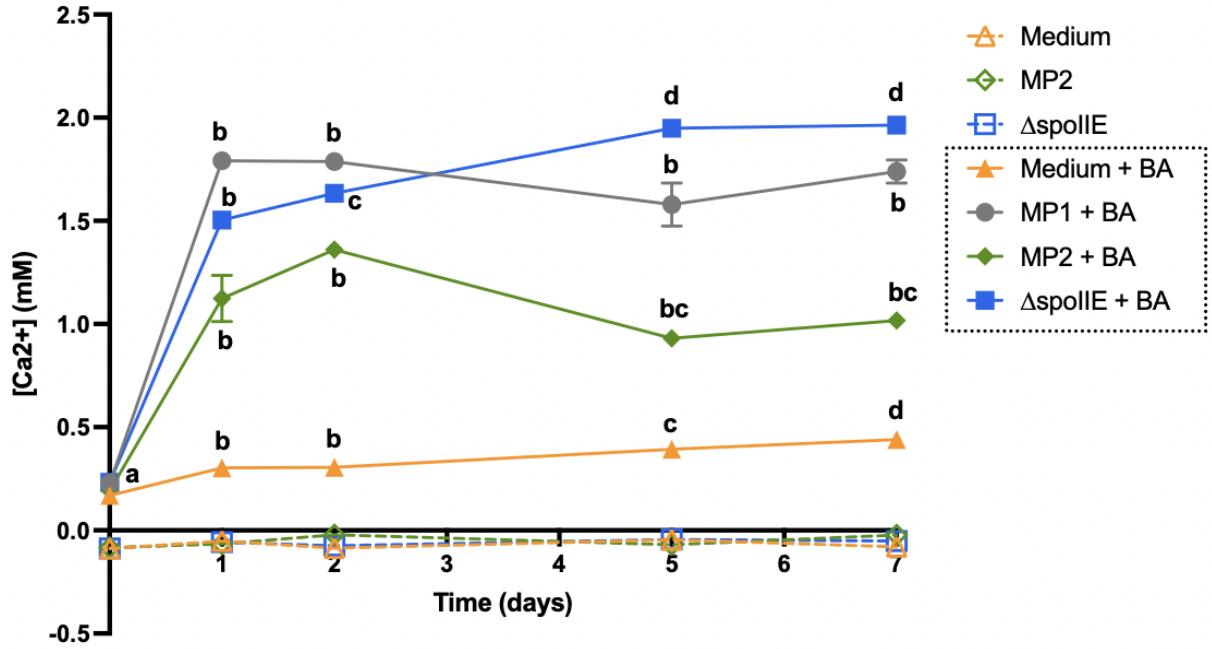

Figure 1. Calcium release during *in vitro* weathering of basalt by *Bacillus subtilis* strains. MP1 (gray circles), MP2 (green diamonds), and a Δ*spoIIE* mutant (blue squares) were cultured in mB4-1 medium with or without basalt (BA) for seven days. Soluble calcium concentrations were quantified at the indicated time points. Data represent the mean +/- SE from biological replicates (n=3). One-way ANOVA and Tukey's multiple comparisons test were performed within each

basalt treatment to determine significant differences among time points. Letters (a, b, c or d) above each time point indicate statistically significant differences ($p < 0.05$).

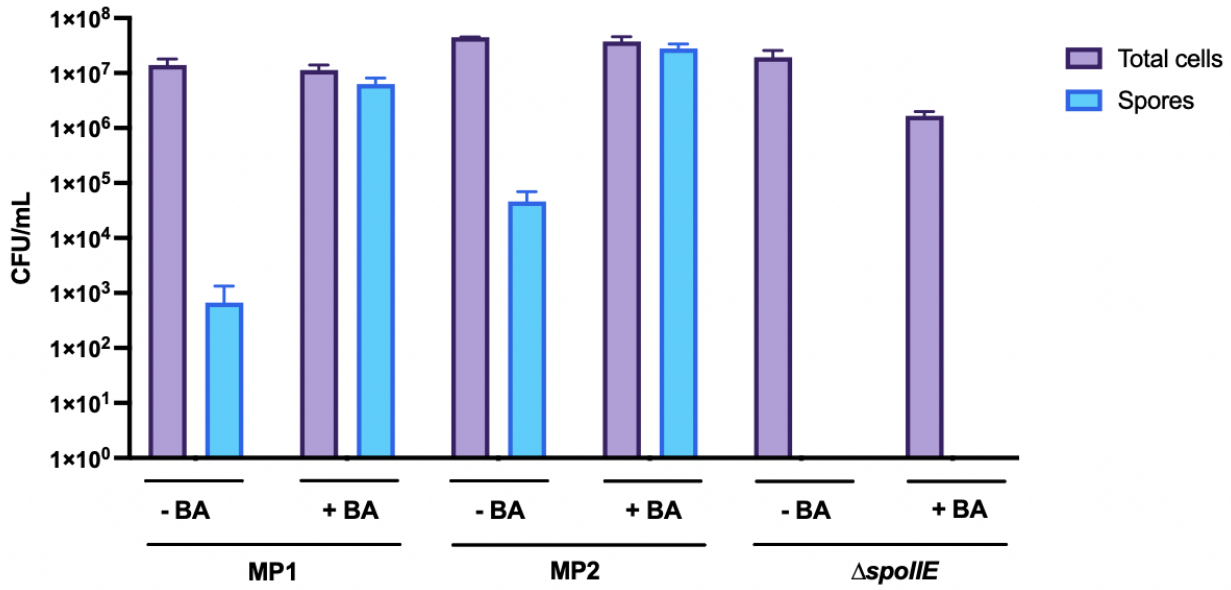

Figure 2. *Bacillus subtilis* strains MP1 and MP2 sporulate under *in vitro* weathering conditions. Total viable cells (purple bars) and spores (blue bars) were enumerated from 3-day cultures grown in mB4-1 medium in the presence (+BA) or absence of basalt (-BA). Data represent the mean +/- SE from biological replicates (n=3).

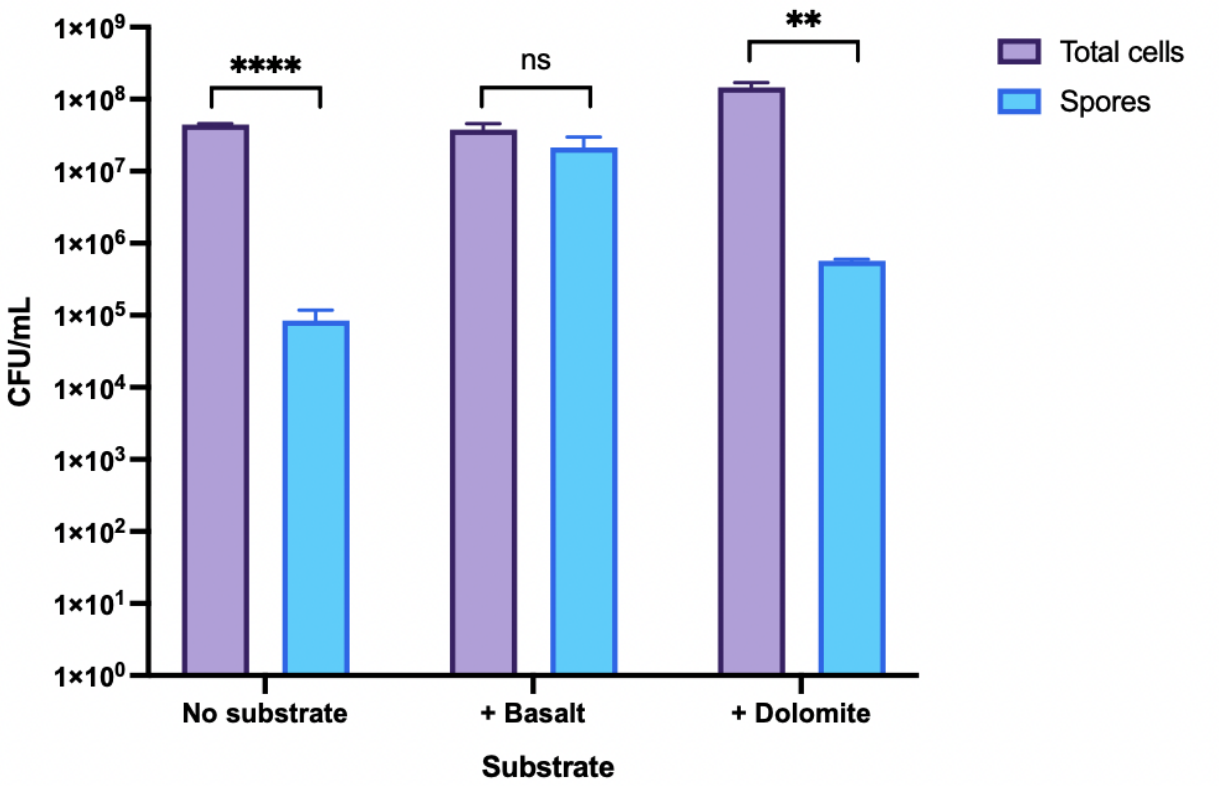

658

659 **Figure 3. Sporulation of *Bacillus subtilis* MP2 in the presence of mineral substrates.** Total
660 viable cells (purple bars) and spores (blue bars) were enumerated from 3-day MP2 cultures grown
661 in mB4-1 medium with or without basalt or dolomite. Data represent the mean +/- SE from
662 biological replicates (n=3). Asterisks above each bar indicate statistically significant differences
663 (unpaired t-test, ns: not significant, ** $p < 0.01$, **** $p < 0.0001$).

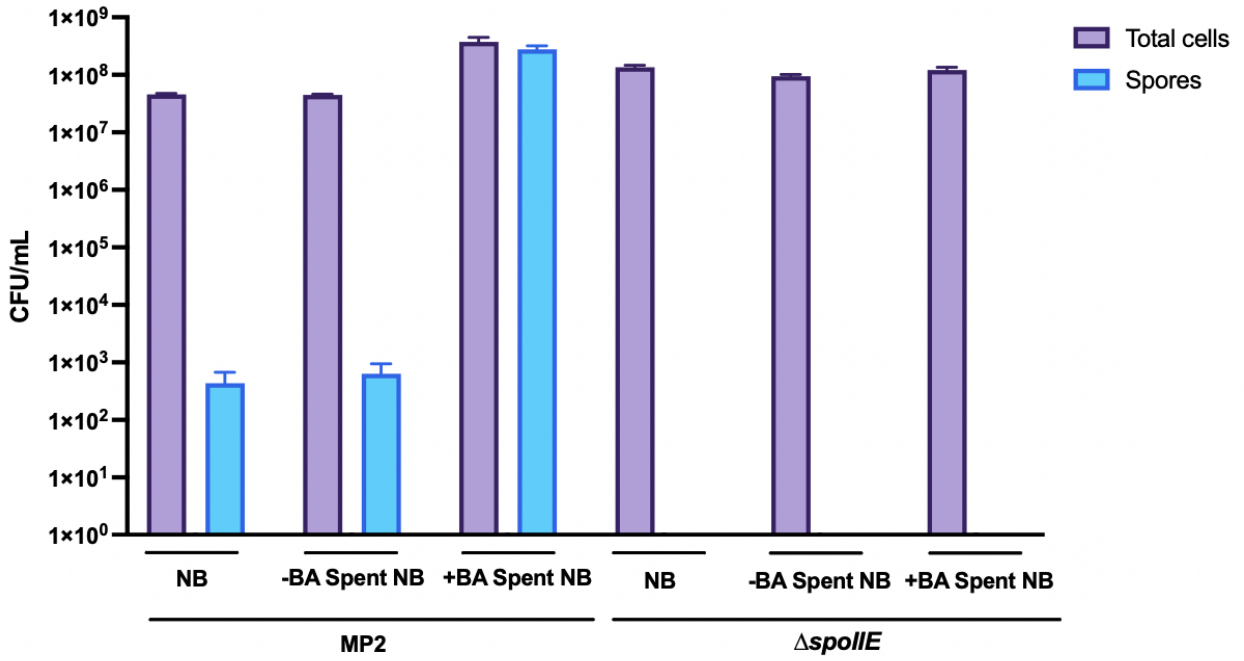

664

665 **Figure 4. Soluble products from basalt incubated with Δ*spoIIE* can induce MP2 sporulation.**

666 Δ*spoIIE* was grown in nutrient broth in the presence (+BA) or absence (-BA) of basalt for 3 days,

667 then the culture supernatants were filter-sterilized to generate spent media (Spent NB).

668 Subsequently, MP2 and Δ*spoIIE* were cultured in fresh nutrient broth (NB), spent NB lacking

669 basalt (-BA Spent NB), and spent NB with basalt (+BA Spent NB). The purple bars represent total

670 cell CFU/ml and the blue bars represent total spore CFU/ml. Δ*spoIIE* produced no spores in any

671 of the conditions tested. Data represents the mean +/- SE from biological replicates (n=3).

672

673

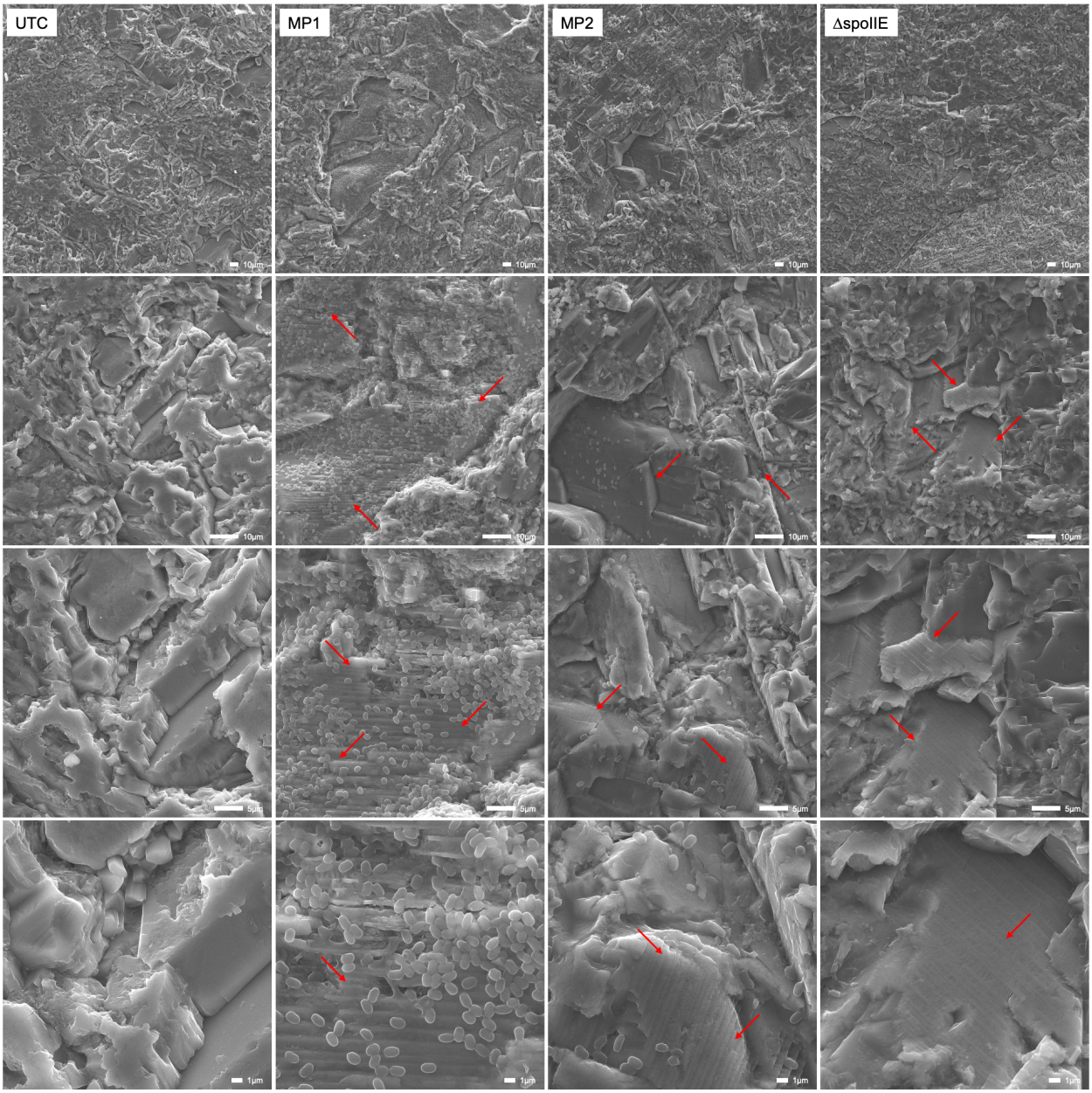

Figure 5. Scanning electron micrographs of basalt surfaces following 30-day incubation with *B. subtilis* strains. Uninoculated basalt disks (UTC) displayed smooth crystalline planes with no visible evidence of microbial colonization. In contrast, basalt surfaces incubated with MP1 and MP2 were densely populated with numerous ovoid spores, visible along striations/crystalline planes (red arrows). The striations closely resemble feldspar twinning, a phenomenon related to geometric crystal growth. Images were acquired at 300x (top row), 1000x (second row), 2000x

(third row), and 4000x (bottom row) magnification. Scale bars = 10 μm (top panel) and 1 μm (bottom panel).

SUPPLEMENTARY INFORMATION

FIGURES AND TABLES

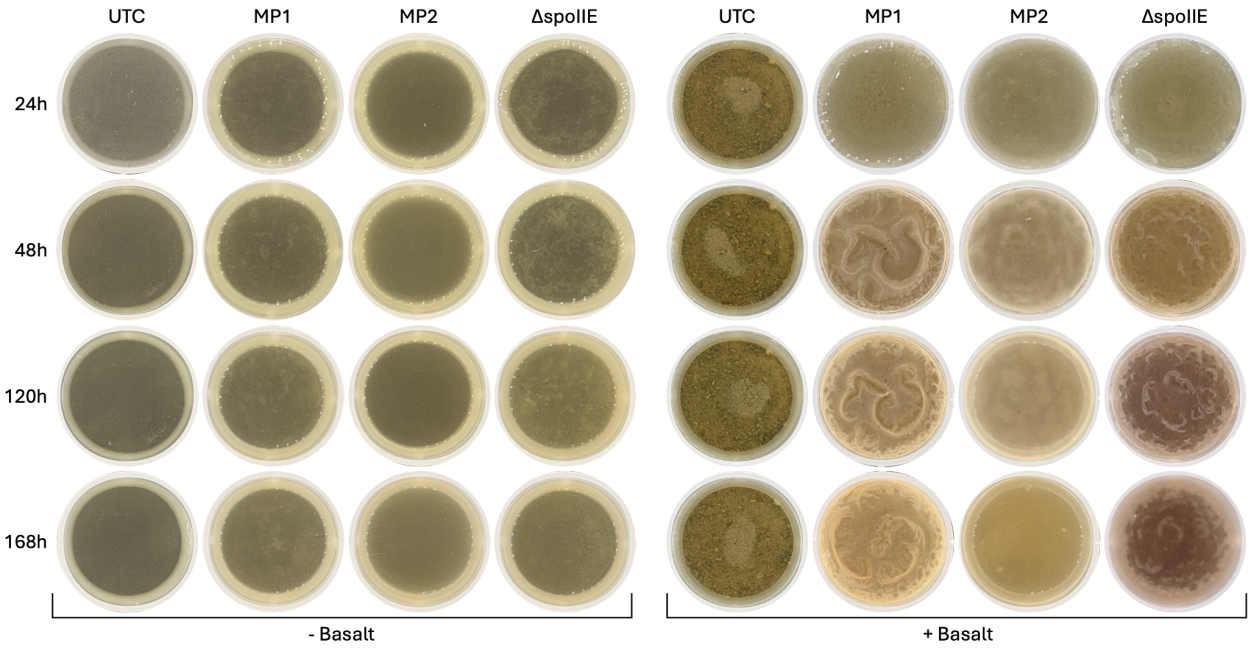

Supplemental Figure S1. *Bacillus subtilis* MP1, MP2, and Δ*spoIIE* growth phenotypes in the presence and absence of basalt. Images of the weathering plates were captured from above at the indicated timepoints. *Bacillus subtilis* MP1, MP2, and Δ*spoIIE* were cultured in mB4-1 in the presence and absence of 50 mg basalt. In the presence of basalt, robust pellicle biofilms were observed after 48-hours.

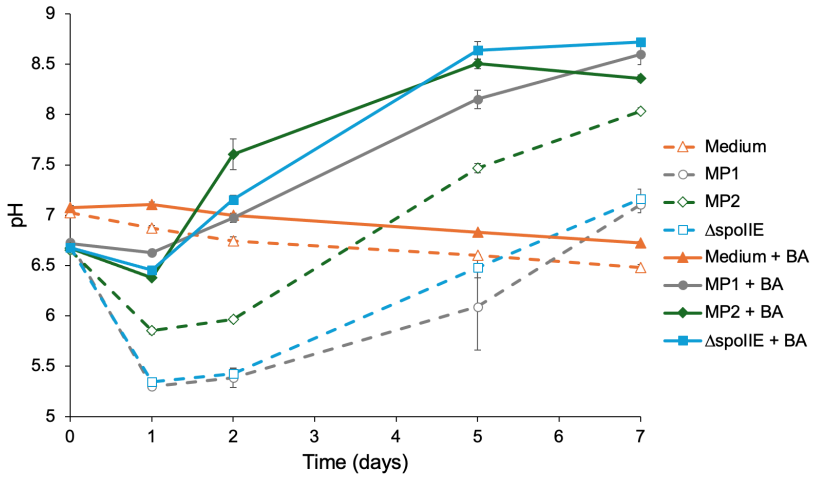

Supplemental Figure S2. pH dynamics during *in vitro* weathering of basalt by *Bacillus subtilis* strains. MP1 (gray circles), MP2 (green diamonds), and a Δ*spoIIE* mutant (blue squares) were cultured in mB4-1 medium with or without (BA) for seven days. The pH of the cultures was measured at the indicated time points. Data represent the mean +/- SD from biological replicates (n=3).

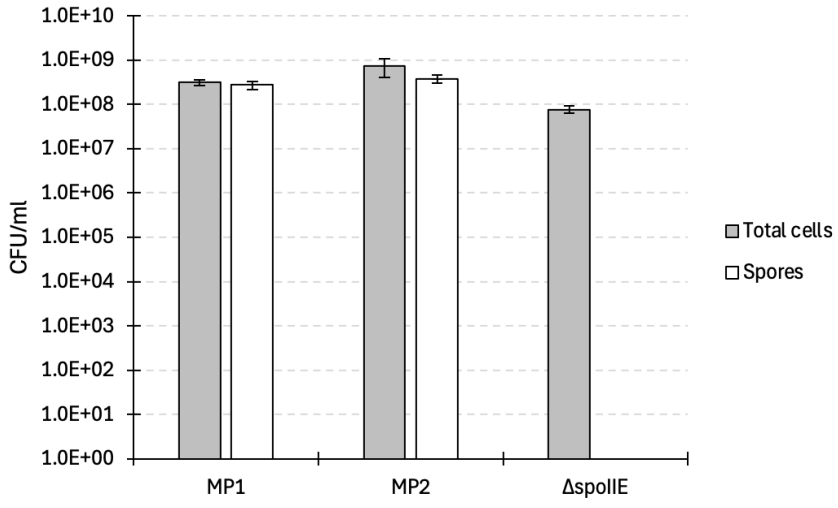

Supplemental Figure S3. *Bacillus subtilis* strains Δ*spoIIE* is impaired in its ability to sporulate while the wild-type strains MP1 and MP2 are not. Total cells and heat-resistant spore

counts after 2 days of incubation in a media that promotes sporulation (DSM). Data represent the mean +/- SD from biological replicates (n=3).

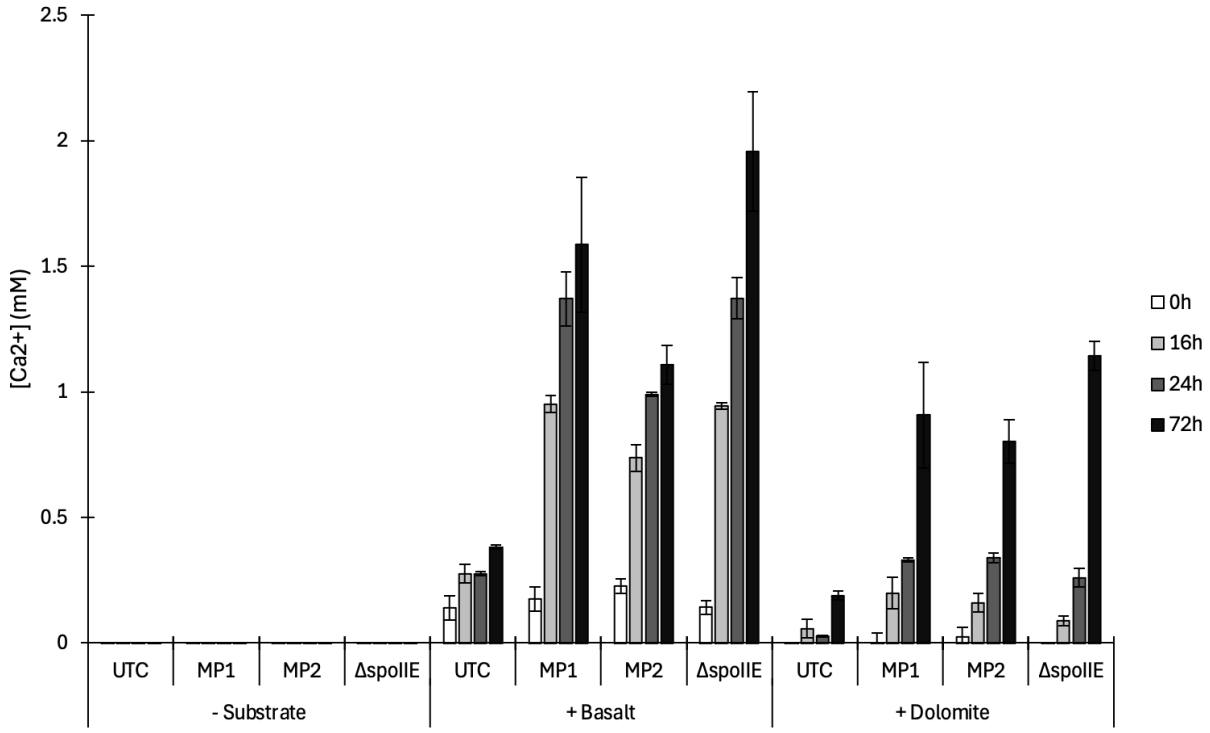

Supplemental Figure S4. Calcium release during *in* vitro weathering of basalt and dolomite by *Bacillus subtilis* strains MP1, MP2, and Δ*spoIIE*. MP1, MP2, and Δ*spoIIE* were cultured in mB4-1 medium with or without basalt and dolomite for three days. Soluble calcium concentrations were quantified at indicated timepoints. MP1, MP2, and Δ*spoIIE* released higher levels of calcium in the presence of both basalt and dolomite. Data represent the mean +/- SD from biological replicates (n=3).

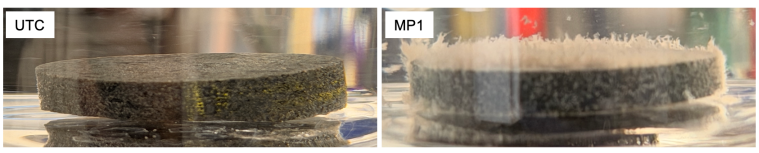

Supplemental Figure S5. Basalt disks after 30-day incubation. Basalt disks resuspended in dH_2O demonstrate dense colonization by MP1, a necessary condition for weathering, as evidenced by the thick biofilm associated with the silicate rock. Biomass and exopolysaccharides associated with biofilms are visually absent from the UTC sample.

Mineral	**Basalt (%)**
Quartz	9
K-Feldspar	0
Albite	0
Other Silicates	0
Pyroxene/Amphibole	28
Anorthite	63

Table S1. The mineral abundance of BrixBlend basalt was measured via semi-quantitative XRD.

Oxide	Basalt (%)
SiO_2	49.1
TiO_2	0.9
Al_2O_3	13.0
FeO*	15.9
MnO	0.2
MgO	6.6
CaO	10.1

Na_2O	2.8
K_2O	0.5
P_2O_5	0.0
LOI %	3.1

Table S2. Elemental abundance of major oxides in BrixBlend basalt measured by XRF. Loss-on-ignition (LOI) represents the mass of volatile compounds in the sample, including organic matter and structural water in clays. *Indicates total iron calculated as FeO.

Sample	**Total Viable Cells (CFU/ml)**	**Total Spores (CFU/ml)**	**Sporulation Frequency (%)**	**Soluble Ca improvement over UTC (%)**
UTC	0.00E+00	0.0E+00	0.0	
MP1	6.02E+07	5.1E+07	82.3	210.1
MP2	7.80E+07	3.7E+07	47.4	126.4
Δ*spoIIE*	6.91E+06	0.0E+00	0.0	109.7

Table S3. Total viable CFUs, spore CFUs, sporulation frequencies, and soluble calcium measurements from 30-day basalt weathering samples.